

Protein Effects on the Electronic Structure of the $[\text{Fe}_4\text{S}_4]^{2+}$ Cluster in Ferredoxin and HiPIP

Thorsten Glaser,[†] Ivano Bertini,[‡] Jose J. G. Moura,[‡]
 Britt Hedman,^{*†§} Keith O. Hodgson,^{*†§} and
 Edward I. Solomon^{*†}

Department of Chemistry
 Stanford University, Stanford, California
 Department of Chemistry
 University of Florence, Florence, Italy
 Departamento de Quimica
 Universidade Nova de Lisboa, Lisboa, Portugal
 Stanford Synchrotron Radiation Laboratory, SLAC
 Stanford University, Stanford, California

Received January 26, 2001

The $[\text{4Fe-4S}]$ cluster core is found in two classes of electron transfer (ET) proteins, namely the 4Fe ferredoxins and the HiPIPs (high potential iron proteins).¹ They are structurally very similar, but exhibit different redox properties. Their functional reduction potentials differ by ~ 1 V. It is well established that these ET proteins utilize different redox couples; $[\text{Fe}_4\text{S}_4]^{2+/1+}$ for the 4Fe ferredoxins and $[\text{Fe}_4\text{S}_4]^{3+/2+}$ for the HiPIPs.² The physical origin of these thermodynamic differences is not known, although a number of possible factors have been proposed³ including the dielectric constant, hydrogen bonding to the sulfur ligands, electrostatic effects from neighboring C=O amide dipoles, water accessibility to the cluster, and the location of the cluster in the protein.

Thus far there has been no experimental estimate of the electronic structures of the $[\text{4Fe-4S}]$ cluster in the protein, thus a determination of the local vs global nature of the effects of the protein on the redox properties. Recently, we have developed ligand K-edge X-ray absorption spectroscopy (XAS) as a direct experimental probe of the covalency of a metal–ligand bond, thus the strength of the bond.^{4a,c} The preedge features of the ligand K-edge are assigned to transitions from the ligand 1s core level to the unoccupied or half-occupied metal d-orbitals which are covalently mixed with the p-orbitals of the ligand. A quantitative analysis of these electric-dipole allowed transitions using the irreducible tensor method yields a direct proportionality between

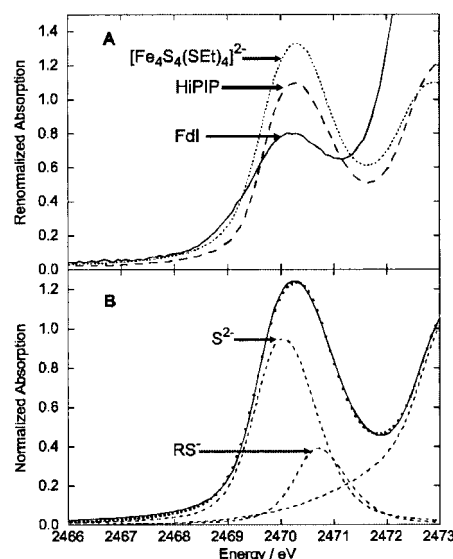


Figure 1. (A) Renormalized S K-edge spectra of FdI from *D. gigas* (solid line), HiPIP from *C. vinosum* (dashed line), and $[\text{PPh}_4]_2[\text{Fe}_4\text{S}_4(\text{SEt})_4]$ (dotted line). The renormalization factors are 12/8 for FdI, 9/8 for HiPIP, and 8/8 for $[\text{PPh}_4]_2[\text{Fe}_4\text{S}_4(\text{SEt})_4]$. (B) Normalized S K-edge spectrum of $[\text{Fe}_4\text{S}_4(\text{SPh})_4]^{2-}$ (solid line) and its simulation (dotted line) using the experimental preedges of $[\text{Fe}_4\text{Se}_4(\text{SPh})_4]^{2-}$ and $[\text{Fe}_4\text{S}_4\text{Cl}_4]^{2-}$ (dashed lines) as thiolate and sulfide contribution, respectively.^{7a}

their intensity and the amount of ligand p-character in the valence orbitals hence the covalency of the metal–ligand bond.^{4a,c} The energy of the preedge is dependent on the effective nuclear charge of the metal (d-manifold binding energy) and the ligand (1s core binding energy) and is thus a probe of the electron density at the different atoms. Here, S K-edge XAS is applied to the $[\text{Fe}_4\text{S}_4]^{2+}$ cluster of HiPIP from *C. vinosum*,⁵ ferredoxin I (FdI) from *D. gigas*,⁶ and the model compound $[\text{PPh}_4]_2[\text{Fe}_4\text{S}_4(\text{SEt})_4]$.⁷ We find a dramatic change in the electronic structure of the $[\text{Fe}_4\text{S}_4]^{2+}$ cluster between the proteins and the model compound, and also between this cluster in HiPIP and FdI. These changes in bonding provide an important contribution to the observed differences in the reduction potential and correlate with differences in hydrogen bonding of the protein backbone to the $[\text{Fe}_4\text{S}_4]^{2+}$ cluster.

HiPIP from *C. vinosum*⁵ and FdI from *D. gigas*⁶ were prepared according to the referenced procedures. The S K-edge spectra were measured at the Stanford Synchrotron Radiation Laboratory using the 54-pole wiggler beam line 6-2.⁸

The appropriate renormalized S K-edge spectra⁹ of the $[\text{Fe}_4\text{S}_4]^{2+}$ cluster from HiPIP, FdI, and $[\text{Fe}_4\text{S}_4(\text{SEt})_4]^{2-}$ are shown in Figure 1A. All spectra exhibit a preedge peak at nearly the same energy (~ 2470.2 eV), however, the intensities of the preedge peaks differ

(5) Bartsch, R. G. *Methods Enzymol.* **1978**, *53*, 329–340.

(6) Bruschi, M.; Hatchikian, E. C.; Le Gall, J.; Moura, J. J. G.; Xavier, A. V. *Biochim. Biophys. Acta* **1976**, *449*, 275–284.

(7) (a) Glaser, T.; Rose, K.; Shadle, S. E.; Hedman, B.; Hodgson, K. O.; Solomon, E. I. *J. Am. Chem. Soc.* **2001**, *123*, 442–454. (b) Hagen, K. S.; Watson, A. D.; Holm, R. H. *J. Am. Chem. Soc.* **1983**, *105*, 3905–3913.

(8) Protein solutions (HiPIP: 2.8 mM in 50 mM potassium phosphate buffer, pH 7.4; FdI: 1.7 mM in 100 mM potassium phosphate buffer, pH 7.6) were measured at ~ 4 °C in a Pt-coated Al block sample holder sealed in front by a 6.35 μm thick polypropylene window. The spectra were measured in a high magnetic field mode of 10 kG with Ni coated harmonic rejection mirror and a fully tuned Si(111) double crystal monochromator, under ring conditions of 3.0 GeV and 50–100 mA. Experimental details are described elsewhere (Hedman, B.; Frank, P.; Gheller, S. F.; Roe, A. L.; Newton, W. E.; Hodgson, K. O. *J. Am. Chem. Soc.* **1988**, *110*, 3798–3805).

(9) Renormalization accounts for sulfur present in the protein which is not bound to the metal cluster and thus contributes to the edge jump but not to the preedge feature. There is a total number of nine sulfurs present in HiPIP and twelve sulfurs present in FdI.

[†] Department of Chemistry, Stanford University.

[‡] Department of Chemistry, University of Florence.

[‡] Departamento de Quimica, Universidade Nova de Lisboa.

[§] Stanford Synchrotron Radiation Laboratory, SLAC, Stanford University.

(1) Beinert, H.; Holm, R. H.; Münck, E. *Science* **1997**, *277*, 653–659.

(2) Carter, C. W., Jr.; Kraut, J.; Freer, S. T.; Alden, R. A.; Sieker, L. C.; Adman, E.; Jensen, L. H. *Proc. Natl. Acad. Sci. U.S.A.* **1972**, *69*, 3526–3529.

(3) (a) Adman, E.; Watenpugh, K. D.; Jensen, L. H. *Proc. Natl. Acad. Sci. U.S.A.* **1975**, *72*, 4854–4858. (b) Kassner, R. J.; Yang, W. *J. Am. Chem. Soc.* **1977**, *99*, 4351–4355. (c) Sheridan, R. P.; Allen, L. C.; Carter, C. W., Jr. *J. Biol. Chem.* **1981**, *256*, 5052–5057. (d) Backes, G.; Mino, Y.; Loehr, T. M.; Meyer, T. E.; Cusanovich, M. A.; Sweeny, W. V.; Adman, E. T.; Sanders-Loehr, J. *J. Am. Chem. Soc.* **1991**, *113*, 2055–2064. (e) Langen, R.; Jensen, G. M.; Jacob, U.; Stephens, P. J.; Warshel, A. *J. Biol. Chem.* **1992**, *267*, 25625–25627. (f) Kodaka, M.; Tomohiro, T.; Okuno, H. *J. Phys. Chem.* **1991**, *95*, 6741–6744. (g) Stephens, P. J.; Jollie, D. R.; Warshel, A. *Chem. Rev.* **1996**, *96*, 2491–1513. (h) Banci, L.; Bertini, I.; Savellini, G. G.; Luchinat, C. *Inorg. Chem.* **1996**, *35*, 4248–4253. (i) Cowan, J. A.; Lui, S. M. *Adv. Inorg. Chem.* **1998**, *45*, 313–350. (j) Babini, E.; Borsari, M.; Capozzi, F.; Eltis, L. D.; Luchinat, C. *J. Biol. Inorg. Chem.* **1999**, *4*, 692–700.

(4) (a) Glaser, T.; Hedman, B.; Hodgson, K. O.; Solomon, E. I. *Acc. Chem. Res.* **2000**, *33*, 859–868. (b) Hedman, B.; Hodgson, K. O.; Solomon, E. I. *J. Am. Chem. Soc.* **1990**, *112*, 1643–1645. (c) Shadle, S. E.; Hedman, B.; Hodgson, K. O.; Solomon, E. I. *J. Am. Chem. Soc.* **1995**, *117*, 2259–2272. (d) Rose, K.; Shadle, S. E.; Eidsness, M. K.; Kurtz, D. M.; Scott, R. A.; Hedman, B.; Hodgson, K. O.; Solomon, E. I. *J. Am. Chem. Soc.* **1998**, *120*, 10743–10747. (e) Rose, K.; Shadle, S. E.; Glaser, T.; de Vries, S.; Cherepanov, A.; Canters, G. W.; Hedman, B.; Hodgson, K. O.; Solomon, E. I. *J. Am. Chem. Soc.* **1999**, *121*, 2353–2363.

Table 1. Energies, Intensities, and Covalencies Obtained from Fits of the Preedge Features of $[\text{Fe}_4\text{S}_4(\text{SEt})_4]^{2-}$, HiPIP, and FdI Using the Preedge Shapes of $[\text{Fe}_4\text{Se}_4(\text{SPh})_4]^{2-}$ and $[\text{Fe}_4\text{S}_4\text{Cl}_4]^{2-}$ as Thiolate and Sulfide References, Respectively

	intensity weighted preedge energy (eV)	intensity	renormalized intensity (dipole strength)	no. of metals bound to the ligand	dipole strength per metal–ligand bond	covalency per metal–ligand bond ^a (%)
$[\text{Fe}_4\text{S}_4(\text{SEt})_4]^{2-}$						
S^{2-}	2470.1	1.29	2.57	3	0.86	39 ± 2
RS^-	2470.8	0.47	0.94	1	0.94	35 ± 2
HiPIP						
S^{2-}	2470.2	0.89	2.00	3	0.66	30 ± 2
RS^-	2470.7	0.42	0.94	1	0.94	35 ± 2
FdI						
S^{2-}	2469.9	0.50	1.49	3	0.50	23 ± 2
RS^-	2470.8	0.27	0.80	1	0.80	30 ± 2

^a For conversion of the experimentally obtained dipole strength into thiolate covalency the blue copper protein plastocyanin is used as reference with a dipole strength of 1.02 corresponding to 38% covalency.¹⁰ Analogously, the infinite chain compound CsFeS_2 is used as reference for the sulfide covalency with an intensity of 1.21 equal to 55.5% sulfide covalency.^{4c} For discussions on error limits see ref 7a.

significantly, with the model compound having the highest intensity and FdI the lowest. The intensity of the preedge feature is proportional to the covalency of the iron–sulfur bond. The different intensities thus reflect a decrease in the covalency of the $[\text{Fe}_4\text{S}_4]^{2+}$ cluster in the protein environment. In addition, the preedges, hence the electronic structures of the $[\text{Fe}_4\text{S}_4]^{2+}$ cluster in HiPIP and FdI, are very different. The preedge feature in all samples is a superposition of the metal-bound sulfide and thiolate ligand features, which are not resolved. These contributions can, however, be distinguished using the experimental preedge features of $[\text{Fe}_4\text{Se}_4(\text{SPh})_4]^{2-}$ and $[\text{Fe}_4\text{S}_4\text{Cl}_4]^{2-}$ as thiolate and sulfide references, respectively. The selenide-substituted compound has only preedge features of a metal-bound thiolate and the chloride-substituted compound has only preedge features of a metal-bound sulfide (Figure 1B). The renormalized sum of these separate edges nicely reproduces that of the $[\text{Fe}_4\text{S}_4(\text{SPh})_4]^{2-}$ model compound, which contains both metal-bound thiolate and sulfide.^{7a} The thiolate and sulfide preedge features represent superpositions of transitions to several final states. The overall shapes of these thiolate and sulfide preedges were thus used to fit the experimental preedges of FdI and HiPIP. During the fitting process, the overall shapes of the thiolate and sulfide preedge features were not changed. This restricted fitting model gave reasonable agreement with the measured preedges (Figure S1). The intensities obtained are converted into covalencies using previously determined correlations.^{4a} The renormalized covalency values (Table 1, last column) correspond to the covalency per metal–ligand bond summed over all metal valence orbitals.

On going from the model compound to the proteins the sulfide covalency decreases from ~40% in the model to ~30% in HiPIP and ~23% in FdI. The thiolate covalency does not significantly change for HiPIP relative to the model, but is reduced from ~35% to ~30% in FdI. These per-bond covalency values give the total covalency per iron center (3 Fe– S^{2-} and 1 Fe– SR^{1-} bond) of ~153% in the model, ~127% in HiPIP, and ~98% in FdI. These covalencies quantify significant changes in the electronic structure of the $[\text{Fe}_4\text{S}_4]^{2+}$ cluster in the different protein environments, as experimentally observed in Figure 1A. The covalency of the

$[\text{Fe}_4\text{S}_4]^{2+}$ cluster in the proteins is reduced as compared to that of the model compound, and there is also a large difference in the electronic structure between FdI and HiPIP. Most of the covalency differences are due to the bridging sulfide ligands and only a moderate change is observed for the terminal cysteine ligands in FdI.

The changes in the local electronic structure of the $[\text{4Fe-4S}]$ cluster between the model and the proteins and between HiPIP and FdI appear to be too large to be associated with more global changes in the dielectric, dipole arrangements, or the location of the iron–sulfur cluster in the protein. Also, slight variations in the orientation of the cysteine ligands should not be responsible for this large difference. The iron–sulfide covalency difference between these cluster sites does, however, correlate with the extent of hydrogen bonding to the cluster. In HiPIP, there is one hydrogen bond to the bridging sulfides and four to the cysteines.¹¹ While there is no structure available for FdI from *D. gigas*, the crystal structure of ferredoxin from *C. acidurici* exhibits three hydrogen bonds to the sulfides and five to the cysteines.¹² All hydrogen bonds are between 3.3 and 3.6 Å.^{11,12} The hydrogen bonds stabilize the electron density on the ligands which reduces their charge donation to the iron centers. This effect is also observed in the rubredoxins⁴ and in 2Fe ferredoxin.¹³ In the latter, the sulfides also show the major covalency decrease. The dramatic effect of hydrogen bonding on the more electron rich sulfide ligation is attributed to its higher charge and larger spatial electron density distribution. The importance of the different amount of hydrogen bonds to the bridging sulfide was also suggested from Resonance Raman studies.^{3d} The contribution of hydrogen bonding to the reduction potential of iron–sulfur proteins has been mainly attributed to electrostatic effects.^{3j} However, S K-edge XAS shows that differences in hydrogen bonding also change the local electronic structure of the $[\text{4Fe-4S}]$ cluster.

In summary, S K-edge XAS shows a large decrease in the covalency of the local iron–sulfur bonding in the $[\text{Fe}_4\text{S}_4]^{2+}$ cluster in protein sites relative to a model compound. The covalency is also reduced in FdI relative to HiPIP. This reduced covalency destabilizes the oxidized relative to the reduced cluster and makes an important contribution to increasing the reduction potential of the active site. These differences in charge donation correlate with the extent of hydrogen bonding, in particular to the bridging sulfides.

Acknowledgment. This research is supported by the NSF (grant CHE-9980549, E.I.S.), the NIH (grant RR-01209, K.O.H.), and PRAXIS (J.J.G.M.). SSRL operations are funded by the Department of Energy, Office of Basic Energy Sciences. The SSRL Structural Molecular Biology Program is supported by the National Institutes of Health, National Center for Research Resources, Biomedical Technology Program, and the Department of Energy, Office of Biological and Environmental Research. We thank Drs. P. Frank and I. Moura for assistance with the protein purification. T.G. thanks the Deutsche Forschungsgemeinschaft for a postdoctoral fellowship.

Supporting Information Available: Spectral deconvolution of spectra (Figure S1) (PDF). This material is available free of charge via the Internet at <http://pubs.acs.org>.

JA0155940

(10) Shadle, S. E.; Penner-Hahn, J. E.; Schugar, H. J.; Hedman, B.; Hodgson, K. O.; Solomon, E. I. *J. Am. Chem. Soc.* **1993**, *115*, 767–776.

(11) Parisini, E.; Capozzi, F.; Lubini, P.; Lamzin, V.; Luchinat, C.; Sheldrick, G. M. *Acta Crystallogr.* **1999**, *D55*, 1773–1784.

(12) Dauter, Z.; Wilson, K. S.; Sieker, L. C.; Meyer, J.; Moulis, J.-M. *Biochemistry* **1997**, *36*, 16065–16073.

(13) Anxolabéhère-Mallart, E.; Glaser, T.; Frank, P.; Hedman, B.; Aliverti, A.; Zanetti, G.; Hodgson, K. O.; Solomon, E. I. *J. Am. Chem. Soc.* Accepted for publication.